12th International Conference on Vibration Problems, ICOVP 2015

Ride Comfort Analysis of Math Ride Dynamics Model of Full Tracked Vehicle with Trailing Arm Suspension

Saayan Banerjee[a], V. Balamurugan[a], R. Krishnakumar[b,*]

[a]*Centre for Engineering Analysis and Design, Combat Vehicles R&D Estt., DRDO, Chennai 600054, India*
[b]*Department of Engineering Design, Indian Institute of Technology Madras, Chennai 600036, India*

Abstract

A detailed ride mathematical model of a full tracked vehicle, consisting of 17 dof, with trailing arm hydro-gas suspensions, is developed. The non-linear coupled governing differential equations of motion are derived for the sprung mass and fourteen unsprung masses, incorporating actual trailing arm kinematics and inertia coupling effects. The non-linear equations are solved using Matlab and validated using a multi-body dynamic model developed in MSC.Adams. Parametric studies and ride analyses have been carried out with different suspension characteristics, over random terrain. This full tracked vehicle mathematical vibration model is generic, computationally efficient and a useful tool for suspension design of tracked vehicles.

Keywords: Tracked vehicle; hydro-gas suspension; multi-body dynamics; ride dynamics

_____

1. Introduction

Due to drastic dynamic operating environment of military tracked vehicles, it is of prior importance to develop the ride dynamics model of tracked vehicles, in order to interpret the vibration magnitudes transferred to chassis. In [1], an in-plane model of tracked vehicle is considered and hydro-gas suspension system has been modeled, using polytropic gas compression law to represent the spring characteristics, and hydraulic conductance law to represent the damper, and validated successfully. Lagrangian formulation of the tracked vehicle, using an arbitrary rigid terrain profile and constant vehicle speed, has been derived in [2]. The track roadwheel-terrain interaction has been taken into account and dynamic analysis as well as ride quality assessment of Armoured Personal Carrier vehicle,

* Corresponding author. Tel: +91-44-2636-3079; fax: +91-44-2638-3661.
  *E-mail address:*saayanbanerjee@cvrde.drdo.in

have been carried out in [2]. However in [1,2], the actual suspension kinematics have been transformed to the equivalent vertical suspension while formulating the governing equations of motion, which may yield some difference as compared to the actual vehicle dynamics with trailing arm suspensions. Moreover, the above studies do not include roll mode of the vehicle. Single station representation of tracked vehicle, incorporating the actual suspension kinematics, has been presented in [3] and bounce dynamic responses have been validated. The process of generation of random road profile from temporal power spectral density, has been described in [4].

From the above studies, it is observed that number of research activities have been undertaken in modeling the tracked vehicle dynamics to understand the vibration levels. The present study has reference to [3] and is focused towards development of the non-linear mathematical ride model of a full tracked vehicle, consisting of 17 degrees-of-freedom with similar hydro-gas suspension characteristics, as described in [3]. The kinematics and non-linear stiffness characteristics of the hydro-gas suspension, as described in section 2.1 [3], is used for developing the ride dynamics model of full tracked vehicle. Initially, static equilibrium configuration of the entire vehicle, has been determined, followed by formulation of the dynamics. Incorporating the trailing arm suspension dynamics in the ride mathematical model, the non-linear coupled governing differential equations of motion have been derived for the sprung mass and fourteen unsprung masses, solved using Matlab and validated through a multi-body dynamic model in MSC.Adams. Thereafter, parametric ride dynamic studies have been carried out with the validated non-linear ride math model over two different types of generated random terrain profiles with specified statistical properties. Ride comfort evaluation has been carried out with different non-linear suspension properties. Random road profiles with specified statistical parameters, have been generated with reference to [4]. This study would predict the vibration levels as the tank negotiates various random terrain conditions and also provide the platform to fine-tune the suspension properties for better ride comfort.

2. Formulation of non-linear vibration model of full tracked vehicle

The vibration model of full tracked vehicle consists of the sprung mass and fourteen unsprung masses, seven on either side of sprung mass. The sprung mass consists of the combined mass of the hull and turret, sprockets, idlers, top rollers and portion of the track above the road-wheels. Each unsprung mass consists of the combined mass of suspension casing and components, axle arm, road-wheel and portion of the track below the road-wheel, lumped at the road-wheel center. Each unsprung mass is connected to the ground through solid tire and track pad, represented as equivalent translational stiffness spring. The tire and track pad damping is neglected.

2.1. Formulation of dynamic equations of motion of full tracked vehicle model

The vibration model of full tracked vehicle consists of 17 degrees of freedom, namely bounce, pitch and roll motion of sprung mass and angular motion of each of the fourteen unsprung masses. 'I' and 'J' represent the sprung mass pitch and roll moment of inertias respectively, about the CG. 'd_{li}' and 'd_{ri}' represent the distance between pivot point of axle arm of left and right side *ith* suspension station and sprung mass CG, measured vertically ($i = 1$ to 7). 'c' represents viscous damping coefficient of the suspensions, along the direction of actuator piston motion. '$\varphi_{li}(t)$' and '$\varphi_{ri}(t)$' represent angular displacements of the unsprung mass, belonging to left and right side *ith* suspension station, with respect to the sprung mass about the axle arm pivot point, from static equilibrium position ($i = 1$ to 7). '$X(t)$', '$\theta(t)$' and '$\phi(t)$' represent the bounce, pitch and roll displacements of the sprung mass respectively, at the sprung mass CG, from static equilibrium position. '$Y_{li}(t)$' and '$Y_{ri}(t)$' represent base excitations from the terrain at bottom of tire spring of left and right side *ith* suspension station ($i = 1$ to 7), respectively. The coordinate system followed for the full tracked vehicle vibration model along with the force and moment representation, has been shown in Fig. 1. The governing differential equations couple the respective degrees of freedom.
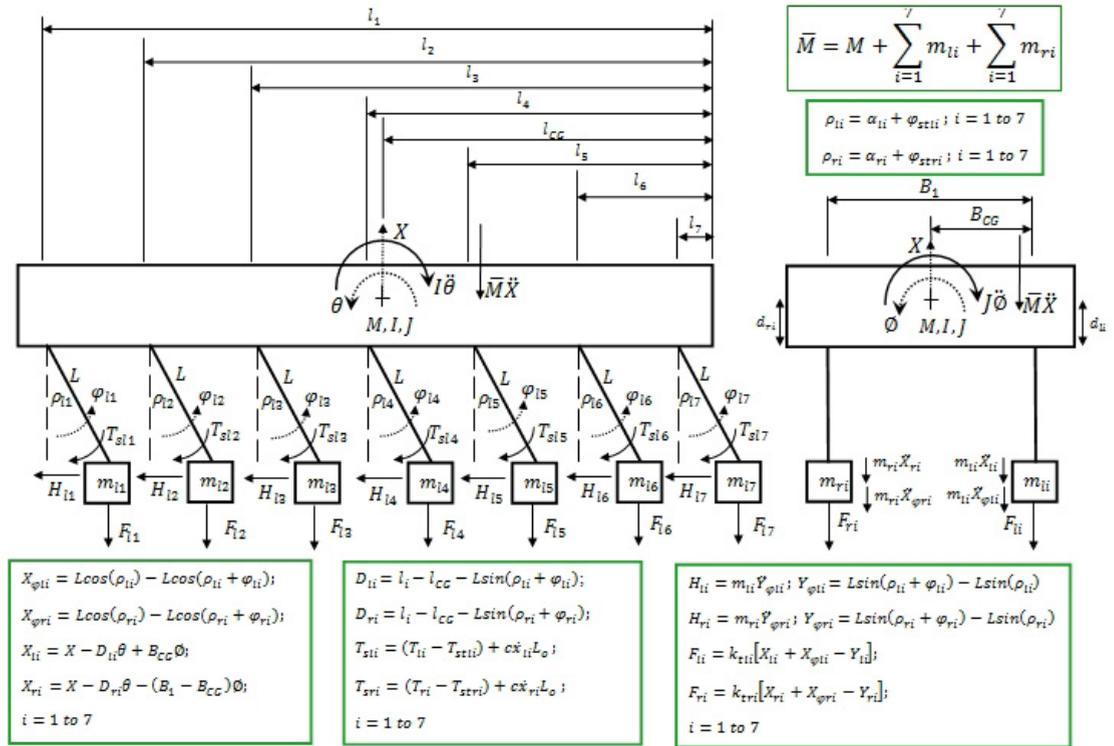
Fig. 1. Representation of forces and moments for full tracked vehicle dynamics

2.1.1. Bounce motion of the sprung mass, measured at sprung mass CG

The second order non-linear coupled governing differential equations of motion, representing bounce motion of the sprung mass (referring to Fig. 1), measured at sprung mass CG, from static equilibrium position, is written as,

$$M\ddot{X} + \sum_{i=1}^{7} m_{li}(\ddot{X}_{li} + \ddot{X}_{\varphi li}) + \sum_{i=1}^{7} m_{ri}(\ddot{X}_{ri} + \ddot{X}_{\varphi ri}) + \sum_{i=1}^{7} F_{li} + \sum_{i=1}^{7} F_{ri} = 0 \tag{1}$$

where,

$M\ddot{X}$ is vertical inertia force of the sprung mass during bounce motion from static position, measured at sprung mass CG.

$m_{li}\ddot{X}_{li}$ and $m_{ri}\ddot{X}_{ri}$ are the vertical translational inertia of the left and right *ith* wheel stations (*i=1 to 7*), due to coupled bounce, pitch and roll motion of sprung mass, measured at sprung mass CG.

$$X_{li} = X - D_{li}\theta + B_{CG}\varnothing \tag{2}$$

$$D_{li} = l_i - l_{CG} - Lsin(\rho_{li} + \varphi_{li}) \tag{3}$$

$$X_{ri} = X - D_{ri}\theta - (B_1 - B_{CG})\varnothing \tag{4}$$

$$D_{ri} = l_i - l_{CG} - Lsin(\rho_{ri} + \varphi_{ri}) \tag{5}$$

$m_{li}\ddot{X}_{\varphi li}$ and $m_{ri}\ddot{X}_{\varphi ri}$ are the vertical components of rotational inertia of the left and right *ith* wheel stations (*i=1 to 7*), measured at sprung mass CG.

$$X_{\varphi li} = Lcos\left(\rho_{li}\right) - Lcos\left(\rho_{li} + \varphi_{li}\right) \tag{6}$$

$$X_{\varphi ri} = Lcos\left(\rho_{ri}\right) - Lcos\left(\rho_{ri} + \varphi_{ri}\right) \tag{7}$$

F_{li} and F_{ri} are the vertical restoring forces from the tire and track pad translational spring, belonging to left and right side *ith* suspension stations (*i* = 1 to 7), measured at sprung mass CG

$$F_{li} = k_{tli}\left[X_{li} + X_{\varphi li} - Y_{li}\right] \tag{8}$$

$$F_{ri} = k_{tri}\left[X_{ri} + X_{\varphi ri} - Y_{ri}\right] \tag{9}$$

2.1.2. Pitch and roll motions of the sprung mass, measured about sprung mass CG

The second order non-linear coupled governing differential equation of motion, representing pitch and roll motions of the sprung mass (referring to Fig. 1), measured about sprung mass CG, from the static equilibrium position, is written as,

$$I\ddot{\theta} - \sum_{i=1}^{7}m_{li}(\ddot{X}_{li} + \ddot{X}_{\varphi li})D_{li} - \sum_{i=1}^{7}m_{ri}(\ddot{X}_{ri} + \ddot{X}_{\varphi ri})D_{ri} + \sum_{i=1}^{7}m_{li}\ddot{Y}_{\varphi li}L_{\varphi li} + \sum_{i=1}^{7}m_{ri}\ddot{Y}_{\varphi ri}L_{\varphi ri}$$
$$- \sum_{i=1}^{7}F_{li}D_{li} - \sum_{i=1}^{7}F_{ri}D_{ri} = 0 \tag{10}$$

$$J\ddot{\varnothing} + \sum_{i=1}^{7}m_{li}(\ddot{X}_{li} + \ddot{X}_{\varphi li})B_{CG} - \sum_{i=1}^{7}m_{ri}(\ddot{X}_{ri} + \ddot{X}_{\varphi ri})\left(B_1 - B_{CG}\right) + \sum_{i=1}^{7}F_{li}B_{CG} - \sum_{i=1}^{7}F_{ri}\left(B_1 - B_{CG}\right) = 0 \tag{11}$$

where,

$m_{li}\ddot{Y}_{\varphi li}L_{\varphi li}$ and $m_{ri}\ddot{Y}_{\varphi ri}L_{\varphi ri}$ are the pitching moments about sprung mass CG due to horizontal components of rotational inertia of the left and right *ith* wheel stations (*i= 1 to 7*).

$$Y_{\varphi li} = Lsin\left(\rho_{li} + \varphi_{li}\right) - Lsin\left(\rho_{li}\right) \tag{12}$$

$$Y_{\varphi ri} = Lsin\left(\rho_{ri} + \varphi_{ri}\right) - Lsin\left(\rho_{ri}\right) \tag{13}$$

$$L_{\varphi li} = Lcos\left(\rho_{li} + \varphi_{li}\right) + d_{li} \tag{14}$$

$$L_{\varphi ri} = Lcos\left(\rho_{ri} + \varphi_{ri}\right) + d_{ri} \tag{15}$$

2.1.3.

Angular motion of the left and right side unsprung masses, measured about pivot location of corresponding axle arm

The second order non-linear coupled governing differential equation of motion (referring to Fig. 1), representing angular motion of each of the left and right side unsprung masses, measured about the axle arm pivot location, from static equilibrium position, are written as,

$$m_{li}L^2\ddot{\varphi}_{li} + m_{li}\ddot{X}_{li}Lsin(\rho_{li}+\varphi_{li}) + (T_{li}-T_{stli}) + c\dot{x}_{li}L_o + F_{li}Lsin(\rho_{li}+\varphi_{li}) = 0 \tag{16}$$

$$m_{ri}L^2\ddot{\varphi}_{ri} + m_{ri}\ddot{X}_{ri}Lsin(\rho_{ri}+\varphi_{ri}) + (T_{ri}-T_{stri}) + c\dot{x}_{ri}L_o + F_{ri}Lsin(\rho_{ri}+\varphi_{ri}) = 0 \tag{17}$$

where,

$m_{li}L^2\ddot{\varphi}_{li}$ and $m_{ri}L^2\ddot{\varphi}_{ri}$ are the rotational inertias of left and right side *ith* unsprung masses about corresponding axle arm pivot location, measured from static equilibrium position. (i = 1 to 7)

T_{li} and T_{ri} are moments resulting from restoring force due to gas spring on actuator piston, about the axle arm pivot location of left and right side *ith* suspension stations, when the axle arm rotates by φ_{li} and φ_{ri} from static position. (i = 1 to 7)

T_{stli} and T_{stri} are moments resulting from restoring force due to gas spring on actuator piston, about the axle arm pivot location of left and right side *ith* suspension stations, at static equilibrium position. (i = 1 to 7)

$\dot{x}_{li}$ and $\dot{x}_{ri}$ are actuator piston velocities for left and right side *ith* suspension stations, measured along the line of motion of the piston, which is a function of the axle arm angular rotation from static position as well as the angular velocity of axle arm, at that particular position. (i = 1 to 7)

Equations (1) to (17) have been coded, solved using Matlab/Simulink and validated through a multi-body dynamic model in MSC.ADAMS. The sprung mass bounce responses, obtained from the math model and MBD model, have been compared in frequency domain and shown in Fig. 2, which shows a close match in dynamics.
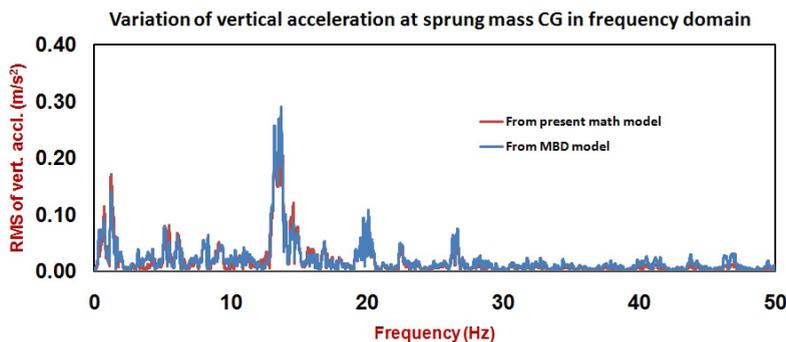

Fig. 2. Bounce acceleration comparative response at sprung mass CG of full tracked vehicle in frequency (for a vehicle speed of 20 kmph over APG terrain)

3. Ride dynamic parametric studies over random terrain

The validated non-linear ride math model for the full tracked vehicle has been simulated over random terrains with specified statistical properties. The temporal power spectral density of various kinds of random roads may be converted to road profile in time domain, assuming the vehicle moving at a particular constant velocity, using the shaping filter method [4]. Consequently, actual road profile in spatial domain is determined from the time domain data. An equivalent multi-body dynamics model of tracked vehicle is developed in Adams Tracked Vehicle (ATV) toolkit of MSC.Adams. The wheel enveloped bases excitation, obtained from ATV, is implemented in the math model, based on the vehicle speed. In the present study, random road profile with variances of 0.064 m^2, corresponding to H class road, as per ISO-8608 standards, have been considered. Vehicle dynamic studies have been carried out over the random road with different non-linear suspension characteristics at defined speeds. Table 1 highlights the magnitudes of various parameters, used for dynamic simulation and ride comfort evaluation.

Table 1. Magnitudes of various parameters

Parameter	Magnitude
M , Sprung mass	50200 kg
I , Sprung mass pitch moment of inertia, about the CG	4.5x10^5 kgm^2
J , Sprung mass roll moment of inertia, about the CG	6.8x10^4 kgm^2
m_{li} and m_{ri} , Unsprung masses on left and right side *ith* suspension station. (i = 1 to 7)	400 kg
k_{tli} and k_{tri} , Translational stiffness of LH and RH ith road-wheel tire with track pads (i = 1 to 7)	8000 kN/m
L , Length of the axle arm of each suspension station	0.55 m
L_0 , Perpendicular distance between the actuator piston and pivot point, for each suspension	0.137 m
l_1 , Dist. between pivot point of axle arm of 1st station and vehicle end.	5.44 m
l_2 , Dist. between pivot point of axle arm of 2nd station and vehicle end.	4.62 m
l_3 , Dist. between pivot point of axle arm of 3rd station and vehicle end.	3.79 m
l_4 , Dist. between pivot point of axle arm of 4th station and vehicle end.	2.97 m
l_5 , Dist. between pivot point of axle arm of 5th station and vehicle end.	2.15 m
l_6 , Dist. between pivot point of axle arm of 6th station and vehicle end.	1.32 m
l_7 , Dist. between pivot point of axle arm of 7th station and vehicle end.	0.50 m
l_{CG} , Dist. between sprung mass CG and vehicle end	2.67 m
B_1 , Dist. between left and right side suspension stations	2.25 m
B_{CG} , Dist. between left side suspension stations and sprung mass CG	1.137 m
α_{li} and α_{ri} , Angle between left and right side *ith* axle arms with the vertical, at rebound position.	20.36 deg (i =1) 32 deg (i = 2 to 7)
d_{li} and d_{ri} , Vert. distance between axle arm pivot points of left and right side ith suspension station and sprung mass CG (i =1 to 7)	0.25 m (*i=1*) 0.3 m (*i*= 2 to 7)
c , Viscous damping coefficient along direction of actuator piston motion	400 kNs/m

3.1. Simulation with suspension charging pressure combination of 85 bar and 75 bar

The non-linear ride mathematical model is subjected to random road excitation with variance of 0.064 m^2 at 35 kmph vehicle speed. The wheel enveloped road excitation, obtained from ATV toolkit of MSC.Adams, is implemented in the math model, based on the vehicle speed. Suspension charging pressure of 85 bar is applied at the 1st, 2nd, 6th, 7th stations LH and RH, and that of 75 bar is applied at the 3rd, 4th, 5th stations LH and RH. The base excitation has been applied such that both tracks of the vehicles are subjected to differential input. Fig. 3 and Fig. 4 show vertical bounce responses at the sprung mass CG and driver's location, in time and frequency domains respectively.
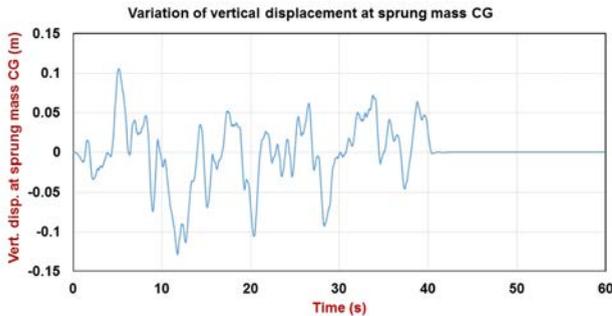

Fig. 3. Bounce displacement response in time domain
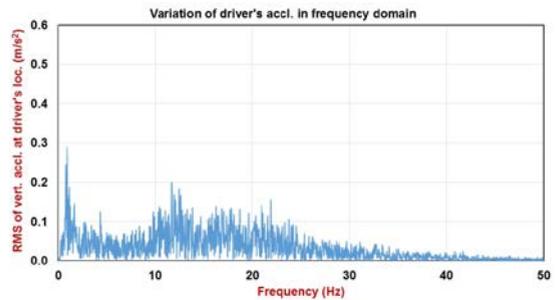
Fig. 4. Bounce acceleration response in frequency domain

3.2. Simulation with suspension charging pressure combination of 110 bar and 105 bar

In the present section, similar math model and vehicle excitation has been applied, as described in section 3.1. However, suspension charging pressure of 110 bar has been applied to the 1st, 2nd, 6th, 7th stations LH and RH, and that of 105 bar has been applied to the 3rd, 4th, 5th stations LH and RH. Fig. 5 and Fig. 6 show vertical bounce responses at the sprung mass CG and driver's location, in time and frequency domains respectively.
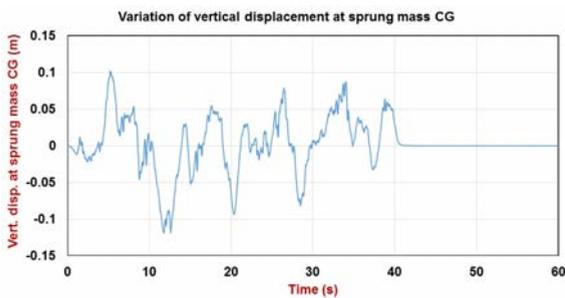

Fig. 5. Bounce displacement response in time domain
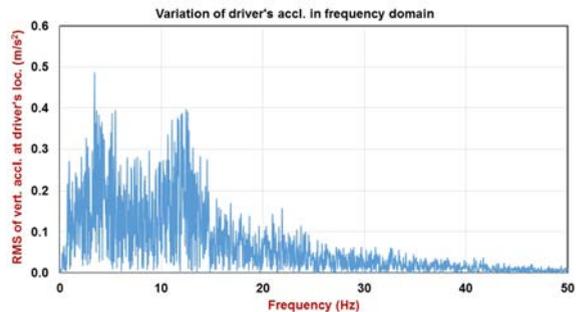
Fig. 6. Bounce acceleration response in frequency domain

Corresponding to vehicle responses, described in sections 3.1 and 3.2, the time domain peak and RMS values of vertical acceleration at the driver's location and that of pitch as well as roll angular acceleration about the sprung mass CG for different suspension characteristics, have been highlighted in Table 2.

Table 2. Summary of results for the vehicle, negotiating random terrain of variance 0.064 m^2 at 35 kmph

Parameter	Suspension charging pressures of 85 and 75 bar		Suspension charging pressures of 110 and 105 bar	
	Peak	RMS	Peak	RMS
Bounce accl. at driver's loc.	1.26 g	0.19 g	2.77 g	0.42 g
Pitch accl. about sprung mass CG	2 rad/s^2	0.29 rad/s^2	4.22 rad/s^2	0.67 rad/s^2
Roll accl. about sprung mass CG	6.55 rad/s^2	1 rad/s^2	12.45 rad/s^2	2.01 rad/s^2

From Fig. 3 and Fig. 5, it is observed that the magnitudes of vertical bounce displacement at the sprung mass CG, are almost of same order for the two suspension configurations. However, it may be noted from Fig. 4 and Fig. 5, that the bounce acceleration response peaks at sprung mass CG, are comparatively higher with increased charging pressures. It may also be noted from Table 2, the driver's bounce acceleration, pitch as well as roll angular acceleration responses about sprung mass CG, are comparatively higher with enhanced suspension characteristics. Vertical acceleration at the driver's location in frequency domain, has been super-imposed over the ISO-2631 fatigue proficiency chart, for suspension charging pressure combination of 85 and 75 bar and also for combination of 110 and 105 bar, and shown in Fig. 7 and Fig. 8 respectively.
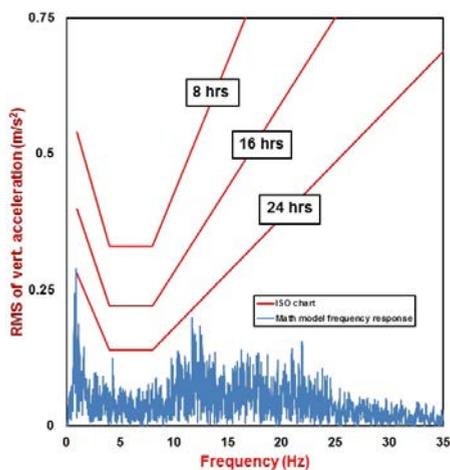
Fig. 7. Bounce accl. response with suspension charging pressure of 85 and 75 bar
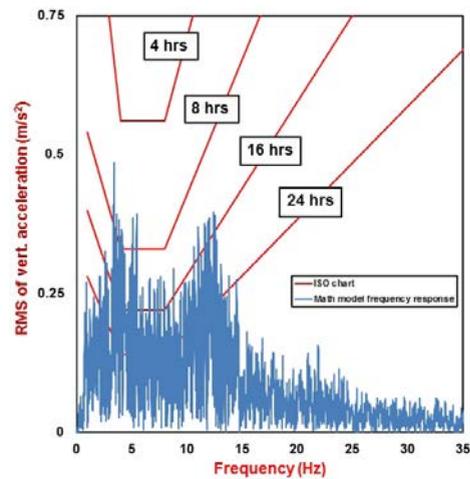
Fig. 8. Bounce accl. response with suspension charging pressure combination of 110 and 105 bar

From Fig. 7 and Fig. 8, it is observed that with suspension charging pressure combination of 85 and 75 bar, the vehicle may negotiate the specified random terrain frequency content for almost 24 hours without driver's fatigue; whereas with suspension charging pressure of 110 and 105 bar, the vehicle may negotiate the specified random terrain frequency content only for 4 hours without the driver's fatigue. Therefore, it is observed that the ride comfort is improved with lower suspension characteristics.

4. Summary and conclusions

The proposed mathematical ride model is a generic one and may be used for ride dynamics study of any tracked vehicle with trailing arm suspensions. The vehicle dynamic analyses have also been further carried out over G class road, where also it was observed that relatively higher suspension charging pressures induce greater vibration transmissibility to the vehicle. The non-linear math model may be used to fine-tune the suspension characteristics and would also be very useful for future semi-active and active suspension design. It may also be noted that the above stochastic excitation studies on the non-linear math model, is computationally much faster, compared to that using multi-body tracked vehicle simulation tools and may easily be implemented in the tracked vehicle simulator.

Acknowledgement

The authors are grateful to Dr. P. Sivakumar, Director, CVRDE and Shri. S. Ramesh, Additional Director (CEAD) for extending all required facilities for carrying out the research work.

References

[1] Solomon, U., Padmanabhan, C: Hydro-gas suspension system for a tracked vehicle: Modeling and analysis. Journal of Terramechanics. 48, 125-137 (2011)
[2] Dhir, A., Sankar, S.: Assessment of Tracked vehicle suspension system using a validated computer simulation model. Journal of Terramechanics. 32 (3), 127-149 (1995)
[3] Banerjee, S., Balamurugan, V., Krishnakumar, R.: Ride dynamics mathematical model for a single station representation of tracked vehicle. Journal of Terramechanics. 53, 47-58 (2014)
[4] Tyan, F., FenHong, H.: Generation of Random road profiles, CSME, ITRI Project: 5353C46000 (1376)